Report
P-20-06
September 2020

Influence of bevel geometry in KBS-3V

Lennart Börgesson
Jan Hernelind

SVENSK KÄRNBRÄNSLEHANTERING AB

SWEDISH NUCLEAR FUEL
AND WASTE MANAGEMENT CO

Box 3091, SE-169 03 Solna
Phone +46 8 459 84 00
skb.se

SVENSK KÄRNBRÄNSLEHANTERING

ISSN 1651-4416
SKB P-20-06
ID 1883219

September 2020

Influence of bevel geometry in KBS-3V

Lennart Börgesson, Clay Technology AB

Jan Hernelind, Scanscot Technology AB

Abstract

An extreme case of having a dry backfill of blocks and pellets in the tunnel and completely water saturated bentonite in the deposition hole all the way up to the tunnel floor, with water freely available along the rock surface is assumed to be the worst case for buffer upwards swelling and has been modelled earlier. The bevel is in the reference case of SKB triangular. However, also a rectangular bevel has been discussed and proposed by Posiva. The effect of changing the bevel from triangular to rectangular has been modelled and analysed in the present report.

Both calculations with the two bevel geometries stopped before complete pore pressure equalisation due to convergence problems. Although the calculations were not run to the end, they could be compared at the same remaining highest suction 150 kPa in the buffer, which occurred at different times. This suction is very low compared to the initial suction at the start of the calculations, which was 18 MPa in the rings and 11 MPa in the blocks. By comparing results at different times at the end of the calculations the conclusion could be drawn that the additional swelling would be small.

The swelling into the rectangular bevel was as expected a little stronger than into the triangular one since the volume of low-density pellets is larger. The maximum horizontal swelling was 26 cm compared to 22 cm. This resulted in a slightly lower density or higher void ratio in the upper part of the deposition hole. It also resulted in a slightly lower vertical stress between the bentonite in the deposition hole and the tunnel (2.7 MPa compared to 2.8 MPa). The differences in results between the two models were generally very small.

The results show that there is an effect of the change to a rectangular bevel, but it is small and not important for the resulting density of the bentonite in the deposition hole.

Sammanfattning

Ett extremfall där en återfyllning av block och pellets i tunneln är helt torr samtidigt som bentonitbufferten i deponeringshålet är helt vattenmättad hela vägen upp till tunnelsulan, med fritt tillgängligt vatten längs bergytan, antas vara det värsta fallet för buffertuppsvällning och har modellerats tidigare. Deponeringshålets avfasning är i SKB:s referensutformning triangulär, men även en rektangulär avfasning har diskuterats och har föreslagits av Posiva. Effekten av att ändra avfasningen från triangulär till rektangulär har modellerats och analyserats i denna rapport.

Båda beräkningarna med de två avfasningsgeometrierna stoppades innan fullständig portryckutjämning på grund av konvergensproblem. Även om beräkningarna inte kördes hela vägen kunde de jämföras vid samma återstående högsta suction 150 kPa i bufferten, som inträffade vid olika tidpunkter.

Denna suction är mycket låg jämfört med den ursprungliga i början av beräkningarna, vilken var 18 MPa i ringarna och 11 MPa i blocken. Genom att jämföra resultat vid olika tidpunkter i slutet av beräkningarna kunde man dra slutsatsen att den kvarstående uppåtsvällningen skulle vara liten.

Uppåtsvällningen i den rektangulära avfasningen var som förväntat lite större än i den triangulära eftersom volymen av pellets med låg densitet är större. Den maximala horisontella buffertuppsvällningen var 26 cm jämfört med 22 cm. Detta resulterade i en något lägre densitet eller högre portal i den övre delen av deponeringshålet. Det resulterade också i en något lägre vertikal spänning mellan bentoniten i deponeringshål och tunnel (2,7 MPa jämfört med 2,8 MPa). Skillnaderna i resultat mellan de två modellerna var i allmänhet mycket små.

Resultaten visar att det finns en effekt av en ändring till en rektangulär avfasning, men den är liten och inte viktig för den resulterande densiteten hos bentoniten i deponeringshålet.

Contents

1 Introduction

One important task for the backfill is to restrict upwards swelling of the buffer in deposition holes. If the buffer can swell upwards it will lose density and by that also important properties. A possible scenario is the so-called dry case of buffer/backfill interaction meaning that the water inflow into the deposition tunnel is very low but at the same time there is a fast wetting of a deposition hole. This means that the buffer in the deposition hole will swell and there will be a pressure build up pushing the dry backfill upwards. The backfill blocks will be piled according to a certain overlapping pattern. The slots between the backfill blocks and the rock will be filled with bentonite pellets and the compression properties of this filling will also influence the ability of the backfill to prevent heaving of the buffer.

Many cases of buffer swelling against both dry and wet backfill have been modelled. The latest modelling results are reported by Börgesson and Hernelind (2018). One of the cases modelled in that report was the extreme case of having a dry backfill of blocks and pellets in the tunnel and completely water saturated bentonite in the deposition hole all the way up to the tunnel floor, with water freely available along the rock surface, was modelled and reported. The bevel in SKB's reference case is triangular. However, also a rectangular bevel has been discussed and proposed by Posiva. The effect of changing the bevel from triangular to rectangular is modelled and analysed in this report.

2 Geometry and material models of the buffer

2.1 Geometry

The model geometries of the deposition hole and the two types of bevel are shown in Figure 2-1.

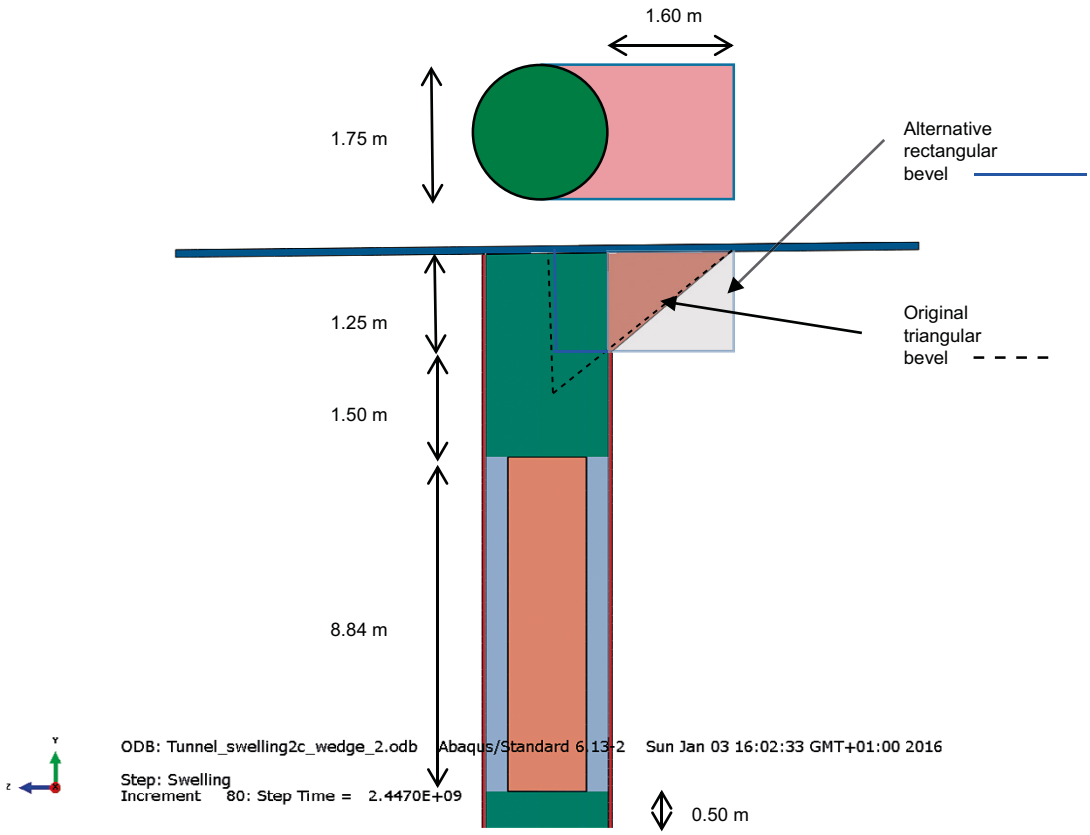

Figure 2-1. *Model geometries. The canister is 1.05 m in diameter and the blocks and rings have an outer diameter of 1.65 m. The tunnel filling is not shown.*

The model geometry of the backfill is shown in Figure 2-2. It is identical to the geometry used for modelling the Buffer swelling test in Äspö HRL and described in Section 3.3.3 in Börgesson and Hernelind (2018).

The thickness of the pellet filling has been set as follows:

- At the crown of the ceiling; 46 cm.
- At the walls; 5 cm.
- At the floor; 10 cm.

The element size of the pellet fillings was about $4 \times 10 \times 10$ cm^3.

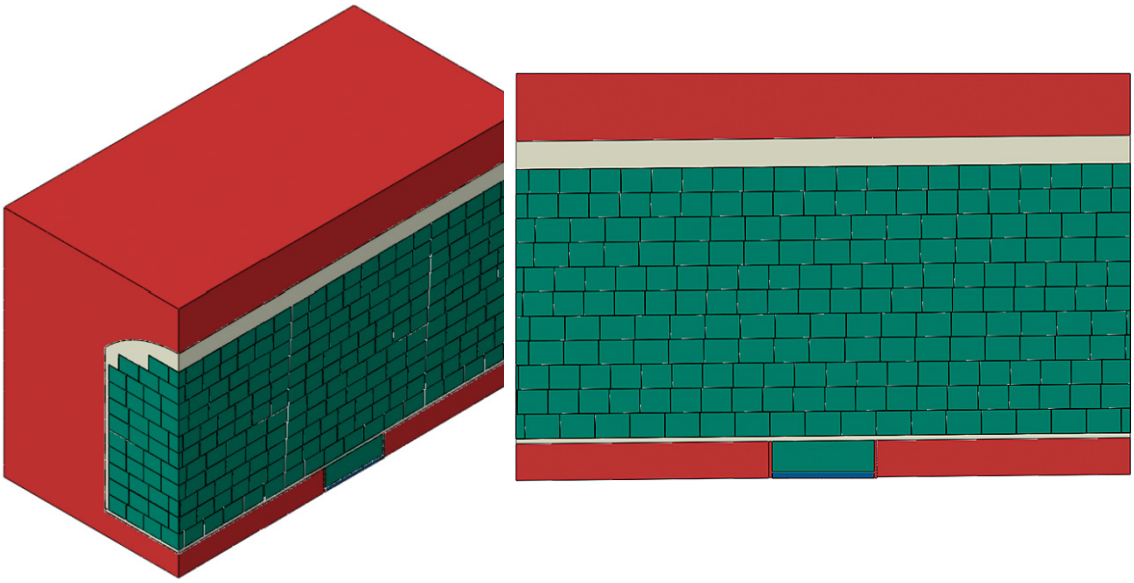

Figure 2-2. *Geometry of the backfill used in the calculation. Each block is one element. The bevel is not shown.*

2.2 Material models

2.2.1 General

The scenario is modelled with the finite element code Abaqus. The code and the material model used for SR-Site are described by Åkesson et al. (2010a, b). The material models used are described in detail by Börgesson et al. (1995). The material models are identical to the models used for the same calculation in Börgesson and Hernelind (2018). The calculation refers to the calculation case 2c described in Section 9.2 of that report (Tunnel_swelling2c_wedge_2).

All bentonite in the deposition hole up to the tunnel floor including the bevel is modelled with pore pressure elements and as completely water saturated from start but with the same initial dry density as planned. All bentonite in the tunnel is modelled without pore pressure elements and thus completely dry with the same dry densities as planned.

2.2.2 The buffer material including the bevel

The material models of the buffer materials are coupled hydro-mechanical with the effective stress theory as base. Full water saturation is assumed for these models. The hydraulic model use Darcy's law with hydraulic conductivity modelled as a function of the void ratio.

The mechanical material model is an elastic-plastic model and uses porous elasticity for the elastic model. The plastic part is a cap model (Claytech plastic cap model) which was calibrated and verified in Task 1 of the homogenisation assignment of TF EBS (Börgesson et al. 2020). The parameter values will be given in this chapter.

Hydraulic model

The applied hydraulic conductivity relation is shown in Table 2-1 (Börgesson et al. 2020).

Table 2-1. Hydraulic conductivity as a function of void ratio.

e	***k*** **(m/s)**
0.45	0.5×10^{-14}
0.70	4.0×10^{-14}
1.00	2.0×10^{-13}
1.5	1.0×10^{-12}
2.00	0.5×10^{-11}
3.00	1.0×10^{-11}
5.00	3.5×10^{-11}
10.00	1.5×10^{-10}
20.00	0.75×10^{-9}

Mechanical models

Porous elastic

Porous Elastic implies a logarithmic relation between the void ratio e and the average effective stress (also called pressure) p according to Equations 2-1 and 2-2.

$$\Delta e = -\kappa \cdot \Delta \ln p \tag{2-1}$$

$$p = (\sigma_1+\sigma_2+\sigma_3)/3-u \tag{2-2}$$

where κ = porous bulk modulus

σ_1, σ_2, σ_3 = principle stresses

u = pore water pressure

Poisson's ratio ν is also required.

$\kappa = 0.175$ (Börgesson et al. 2020)

$\nu = 0.3$

This relation is not valid for low densities (see Börgesson et al. 1995) but only in the interval $0.7 < e < 1.5$, which correspond to 1 110 kg/m^3 $< \rho_d <$ 1 635 kg/m^3. At lower densities the porous bulk modulus is much larger ($\kappa \approx 1.37$) but this change in modulus is not included in the model. If swelling causes a lower density the swelling will not be correctly modelled for that part.

Claytech plastic cap model

This model and its background are described in detail in Börgesson et al. (1995, 2018). The model is illustrated in Figure 2-3.

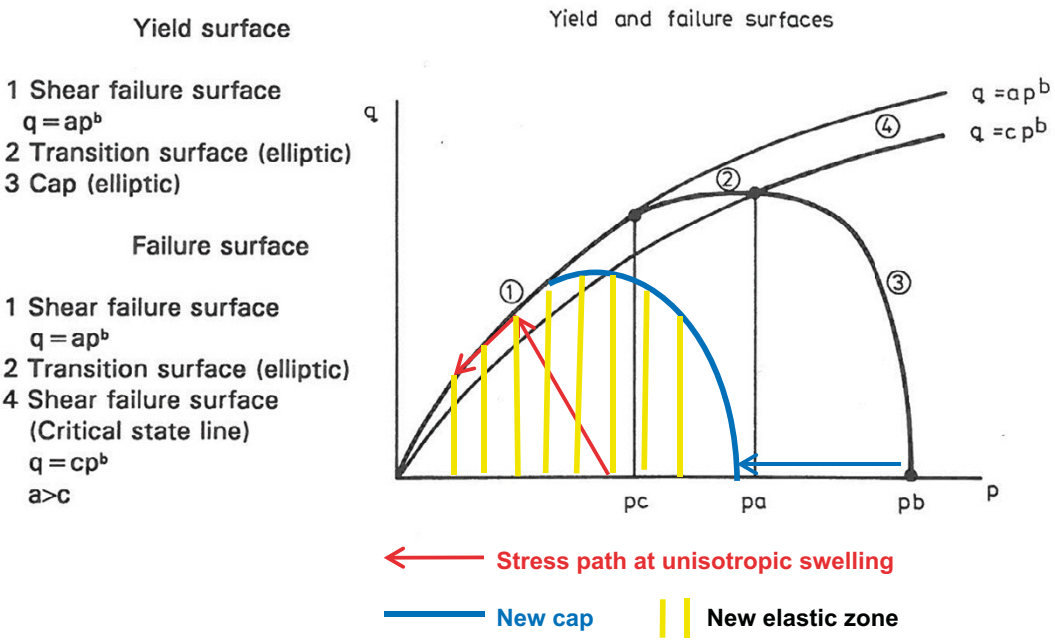

Figure 2-3. *Illustration of the plastic cap model and the consequence of nonisotropic swelling.*

The calibrated parameters of the model (Börgesson et al. 2020) are

Claytech plastic cap model

a = 2.45

c = 2.20

b = 0.77

K= 1.0

γ = 0.2

R = 0.1

p_b = 30 000 kPa

p_f = −25 000 kPa

Cap hardening = see Table 2-2

Table 2-2. Cap hardening function.

p kPa	$e_{\log(1+\varepsilon^{v}_{pl})}$
100	0
331	0.1133
934	0.2112
2 160	0.2904
3 247	0.3289
4 294	0.3553
8 240	0.4169
10 044	0.4356
12 530	0.4565
13 299	0.4621
17 562	0.4884
30 000	0.5390

Contact properties

The contacts between the buffer materials and the rock or canister have been modelled with contact surfaces with a friction angle acting between the materials. The shear resistance between the bentonite and steel has been investigated with a large number of friction tests (see e.g. Börgesson et al. 2020). The friction angle varies with the swelling pressure and the smoothness of the surface.

The friction angle of bentonite varies between 9 and 15 degrees at swelling pressures below 5 MPa. Between bentonite and a smooth surface of steel it is about half the inner friction of bentonite while it is equal to the inner friction of the bentonite if the surface is very raw. The friction angle can thus vary between 4.5 and 15 degrees depending on the swelling pressure and surface properties.

For the calculations of the buffer/backfill interaction the following friction angle ϕ_c has been used:

ϕ_c = 8.69º

The friction angle 8.69° corresponds to an average between bentonite and raw and smooth surfaces at the actual swelling pressures 0.5–5 MPa.

Other materials in the deposition hole

The canister is modelled as a hydraulically impermeable very stiff elastic monolete that is free to move axially.

The rock is modelled as a hydraulically impermeable very stiff elastic material that is fixed.

2.2.3 The backfill

The backfill including the pellet filling in the floor is modelled without pore pressure elements since it is dry and not effected by water. Only mechanical models are applied.

There were three different parts included in the dry backfill, namely the blocks, the joints between the blocks and the pellet filling. The models are identical to the models used for modelling the buffer swelling test described in Börgesson and Hernelind (2018, Section 3.3). The properties of the backfill and the modelling technique were verified by comparing with the results from that test.

Block section of masonry

The backfill blocks were modelled as a linear elastic material with the following properties

E = 245 MPa

ν = 0.17

Initial average stress p_0 = 0 MPa

Although the blocks used in the test differed somewhat from the reference blocks (mainly by having a lower dry density) the properties of the reference blocks were used as the base case. Each block was modelled with one element.

Pellet section

The parts filled with pellets were modelled with linear elasticity and Drucker-Prager plasticity. The plastic behaviour was modelled with Drucker-Prager plasticity.

Drucker-Prager plasticity

β = friction angle in the p-q plane

δ = cohesion in the p-q plane

Ψ = dilation angle

$q = f(\varepsilon^d_{pl})$ = yield function

β = 55° (corresponds to a Mohr-Coulomb friction angle of ϕ = 30°)

δ = 0.052 kPa (intercept on q-axis (p = 0))

ψ = 0° dilatancy

Yield function (ideally plastic at the yield surface).

q (kPa)	ε_{pl}
0.1	0

Elastic properties

E = 3.9 MPa (base case)

ν = 0.3

Initial average stress p_0 = 0 MPa

The properties correspond to the properties of a pellet filling that has not been compacted.

Joints between blocks

Since the bottom bed on which the blocks rest cannot be made as a completely plane or horizontal surface the backfill blocks will be placed slightly uneven in relation to each other. This means that there will be joints that are not even due to slightly inclined blocks that also have slightly different heights. The properties of these joints between the blocks are not well known but they will have compression and friction properties that deviate significantly from the properties of the blocks.

The following properties were applied to the joints (both horizontal and vertical):

- Average joint thickness; 4 mm (fictive).
- Compression properties; the joints are closed at an external pressure of 10 MPa.
- Friction angle $\phi = 20°$.

Figure 2-4 shows the stress-compression relation that has been used for the joints.

The joint is a contact surface property where the contact pressure is defined versus the normal vertical displacement. The joint is seemingly closed at 4 mm displacement corresponding to the normal pressure 10 MPa but if the pressure exceeds 10 MPa the compression will continue. However, the actual pressure will never be near such a high value.

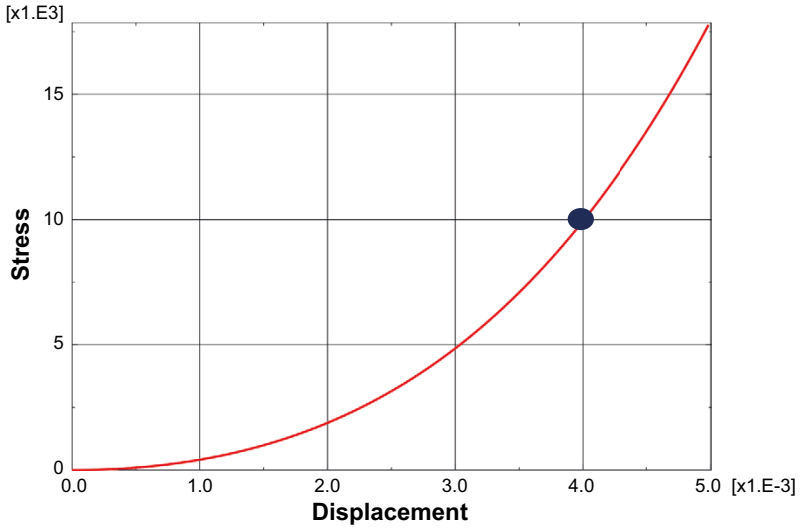

Figure 2-4. *Mechanical model of the joints between blocks. The displacement or compression (m) of the joint is plotted as a function of the total stress (kPa) perpendicular to the joint. After 4 mm compression the 4 mm joint is closed at the stress 10 MPa.*

Rock

The rock was modelled as an elastic material with high stiffness, which means that it only works as a boundary.

Contact properties

The contact between the pellets filling and the rock was not tied in order to allow slip. Instead interface properties with a specified friction were applied between the different materials. The friction was modelled with Mohr Coulomb's parameter friction angle ϕ and without cohesion c.

$\phi = 30^{\circ}$

$c = 0$

This friction angle corresponds to the friction angle of the pellets filling $\beta = 55°$ in the Drucker-Prager model, which means that the contact surfaces are considered rough.

The contact surfaces were made not to withstand tensile stress, which means that the contact may be lost, and a gap formed between the surfaces.

2.2.4 Boundary conditions

Hydraulic boundary

The interface between the deposition hole walls and the rock is modelled with a constant pore water pressure that is ramped to $u = 0$ MPa in a couple of days. This interface includes the bevel and the deposition hole up to the tunnel floor.

Mechanical boundary

The rock is mechanically fixed to the surroundings. All vertical boundaries of the entire model are modelled as symmetry planes.

The interfaces between rock and the buffer, the backfill and the pellet fillings are modelled with contact surfaces as described earlier.

2.3 Initial conditions

The calculation refers to the corresponding calculation 2c described in Section 9.2 of Börgesson and Hernelind (2018) with the triangular bevel. The initial conditions of the bentonite in the deposition hole are shown in Table 2-3.

Table 2-3. Initial conditions of the buffer parts.

Blocks			
Case	**Void ratio e_0**	**Pressure p_0 and Pore pressure $-u_0$ (MPa)**	**Remarks**
(2) 7 MPa	0.683	10.9	Recalculated[1]
Rings			
Case	**Void ratio e_0**	**Pressure p_0 and Pore pressure $-u_0$ (MPa)**	**Remarks**
(2) 7 MPa	0.591	18.4	Recalculated[1]
Pellet filling in the deposition hole and the bevel			
Case	**Void ratio e_0**	**Pressure p_0 and Pore pressure $-u_0$ (MPa)**	**Remarks**
1–3	1.78	0.022	Recalculated[1]

[1)] Recalculated means that the pressure p_0 has been adapted to the yield the correct swelling pressure at the desired average density. This must be done for the blocks and the pellets since the validity of the Porous Elastic model is limited to $0.7 < e < 1.5$. See Börgesson and Hernelind (2018, Section 5.2.2) for further information.

3 Results

3.1 General

The final results from the new calculations with rectangular bevel will be shown as well as corresponding results from the calculations with the triangular bevel. Since there were large problems with convergence for both calculations none of them was possible to run to complete equilibrium with zero negative pore water pressure in the entire buffer. The calculation with the triangular bevel reached the smallest negative pore pressure (−60 kPa) while the calculation with rectangular only reached −150 kPa. The difference is small and considering that the initial pore pressure in the rings are −18 400 kPa, equilibrium is very close.

However, in order to have an as accurate comparison as possible, the calculation with the triangular bevel was repeated with results plotted for the same pore pressure as for the rectangular bevel.

In order to see the influence of the final pore pressure the results of the triangular bevel at the highest suction 150 kPa and the results at the highest suction 60 kPa will also be compared.

3.2 Results for the rectangular bevel and comparison

The results at the highest negative remaining pore pressure −150 kPa is compared. Figures 3-1 to 3-6 show the results in the buffer and the bevel for both cases for comparison. Figures 3-7 and 3-8 show results in the backfill.

Figure 3-1 shows the pore pressure distribution for the two cases at the time where the comparison is done. The elapsed time at that situation was about 2.75×10^9 seconds or 87 years for the calculation with a triangular bevel and 3.19×10^9 seconds or 101 years for the calculation with a rectangular bevel. The longer time required for the rectangular bevel is judged to mainly be caused by the larger volume of bentonite in the bevel and the longer distance to the rock surface.

Figure 3-1 shows that the remaining pore water pressure distribution is very similar for the two cases.

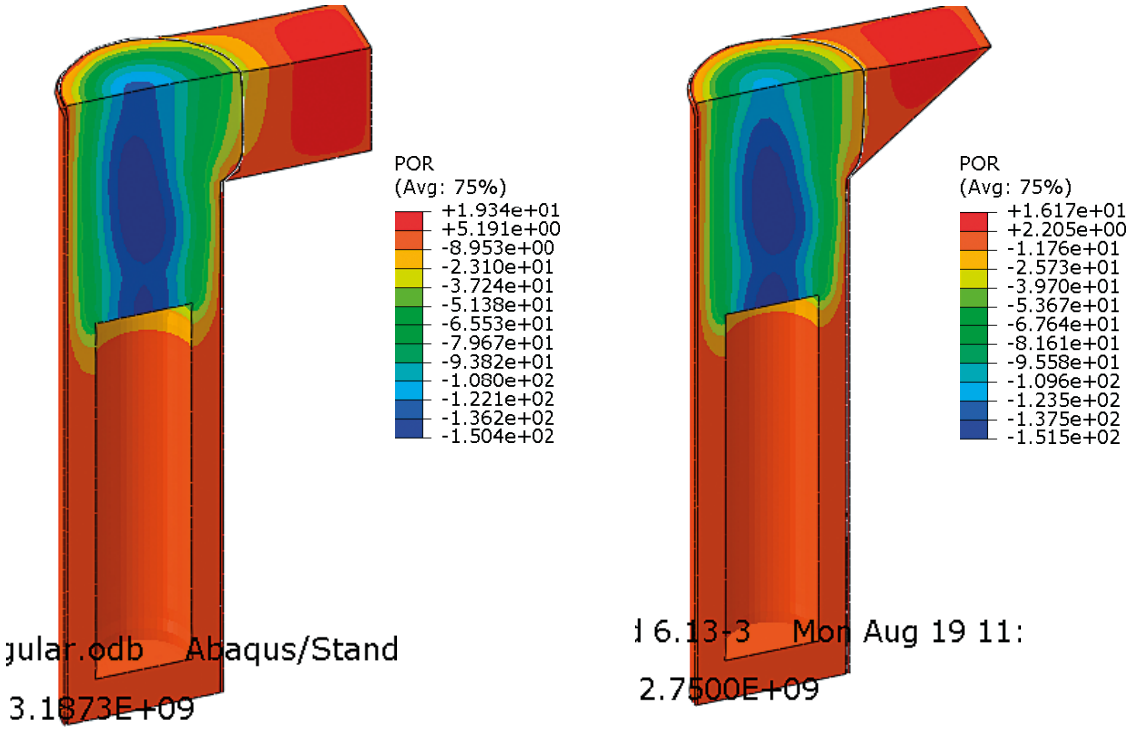

Figure 3-1. *Remaining pore water pressure distribution (kPa) at the time when the comparison is done.*

Figure 3-2 shows the horizontal displacements.

The comparison shows that the horizontal swelling of the buffer into the bevel is (as expected) somewhat larger for the rectangular bevel that for the triangular one (26 cm compared to 22 cm). The loss in density in the deposition hole will thus be a little higher.

Figure 3-3 shows the vertical displacements.

Figure 3-3 shows that also the maximum upwards swelling is a little larger for the rectangular bevel (about 12 cm compared to 11), which could be a little surprising since the density should be a little lower in the upper part of the deposition hole due to the larger horizontal swelling. However, a closer look at the displacement results shows that the largest displacements in the rectangular case takes place locally in the corner of the bevel as market in the figure.

Figures 3-4 to 3-6 show vertical total stresses, dry density and void ratio for the two cases. They all show very similar results but with slightly lower density and vertical stress for the rectangular case.

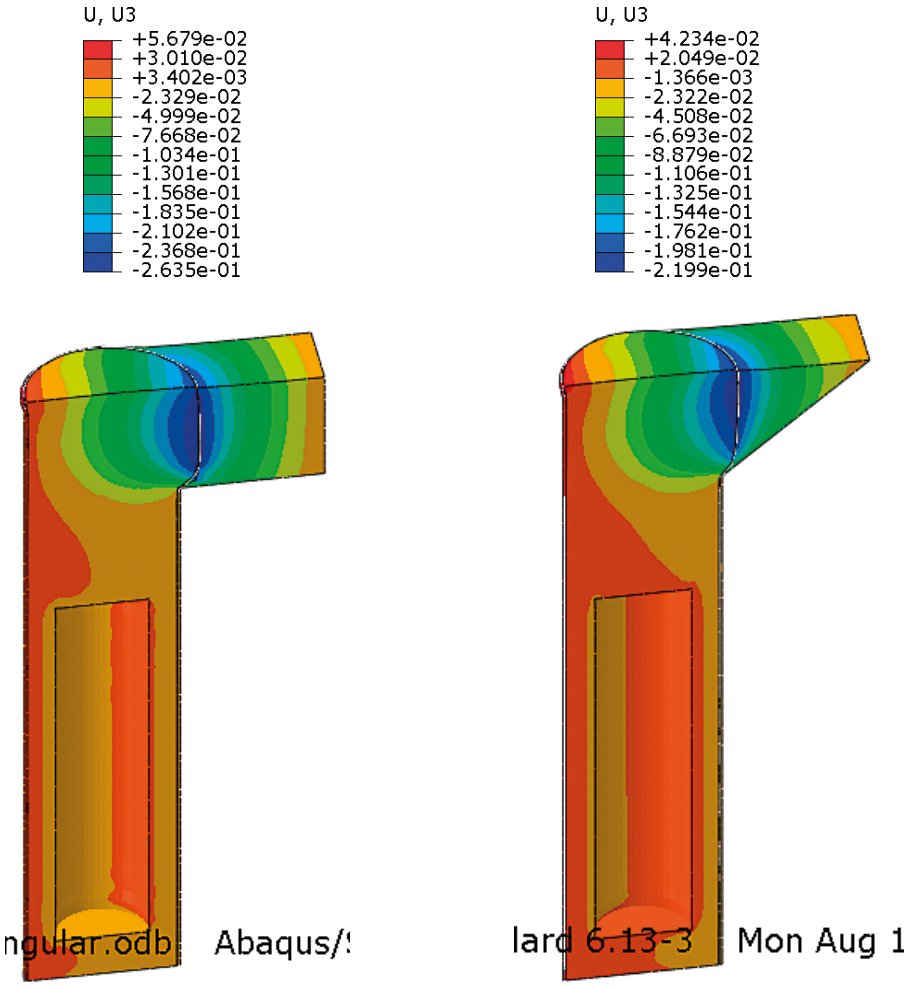

Figure 3-2. *Horizontal displacements (m).*

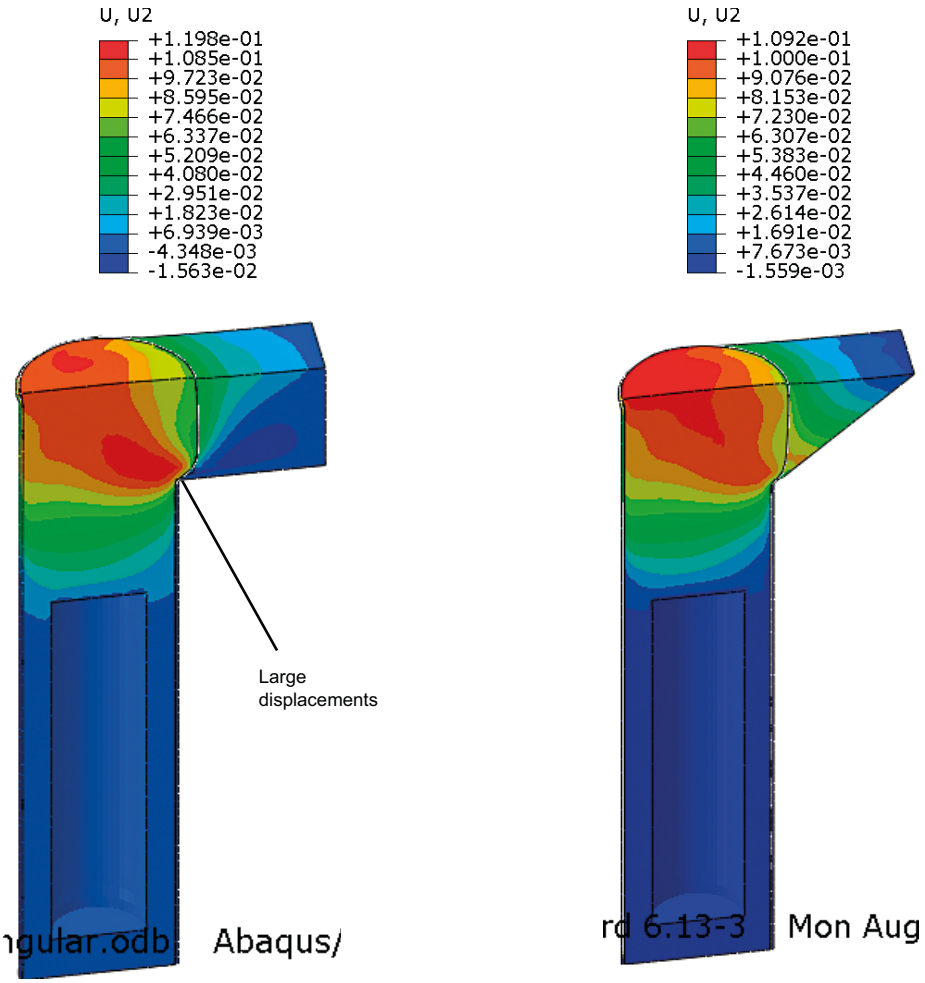

Figure 3-3. *Vertical displacements (m).*

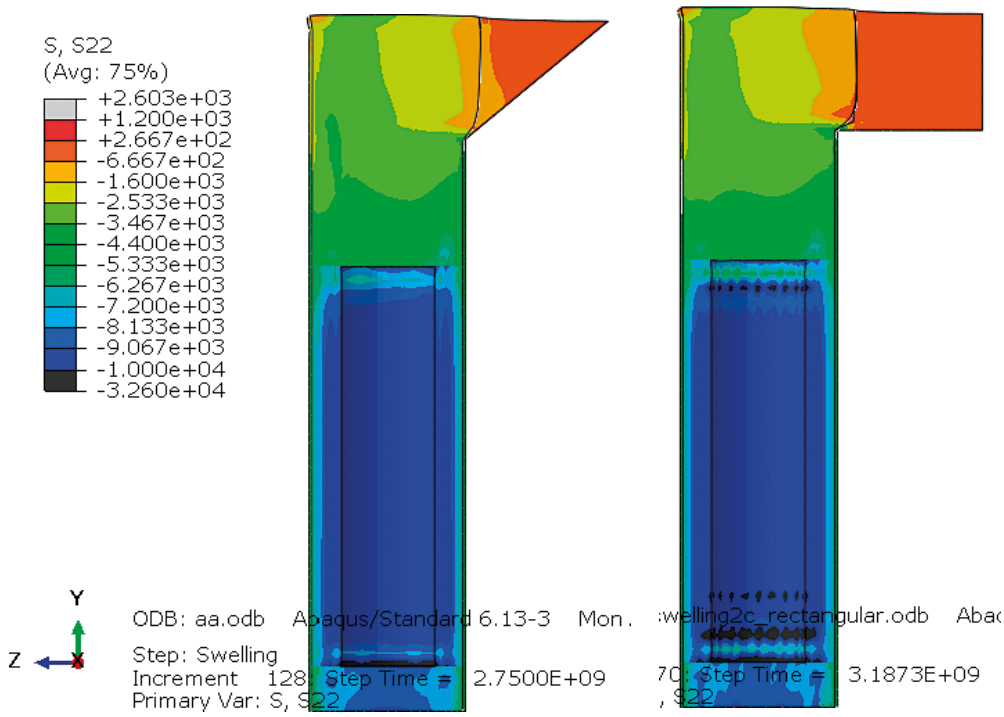

Figure 3-4. *Vertical total stress (kPa).*

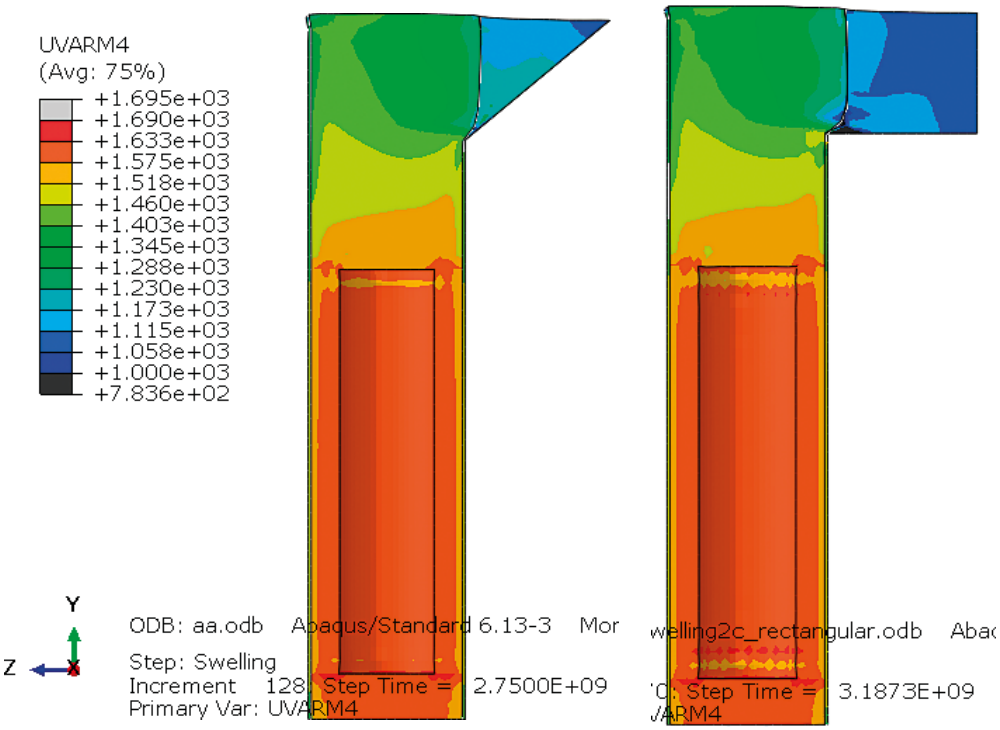

Figure 3-5. *Dry density (kg/m³).*

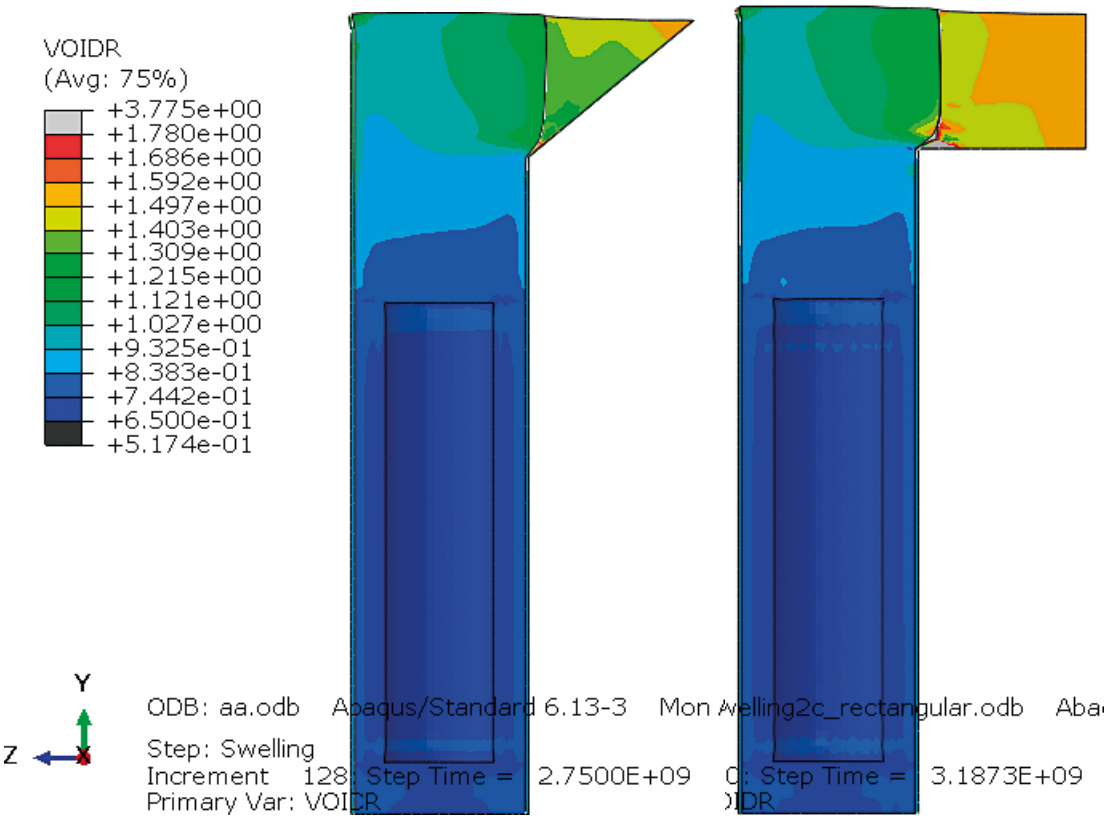

Figure 3-6. *Void ratio (-).*

Figure 3-7 shows the vertical total displacements in the backfill and Figure 3-8 the vertical stress.

The maximum displacements are about 11 cm at the contact between the bentonite in the deposition hole and the bentonite in the backfill for both cases, which agrees with the maximum displacements in the buffer in contact with the backfill. The apparent difference in colour in a large part of the backfill is due to the difference in colour at zero displacement.

The maximum vertical stresses are about 2.8 MPa at the contact between the bentonite in the deposition hole and the bentonite in the backfill for both cases, which agree with the maximum vertical stresses in the buffer shown in Figure 3-4.

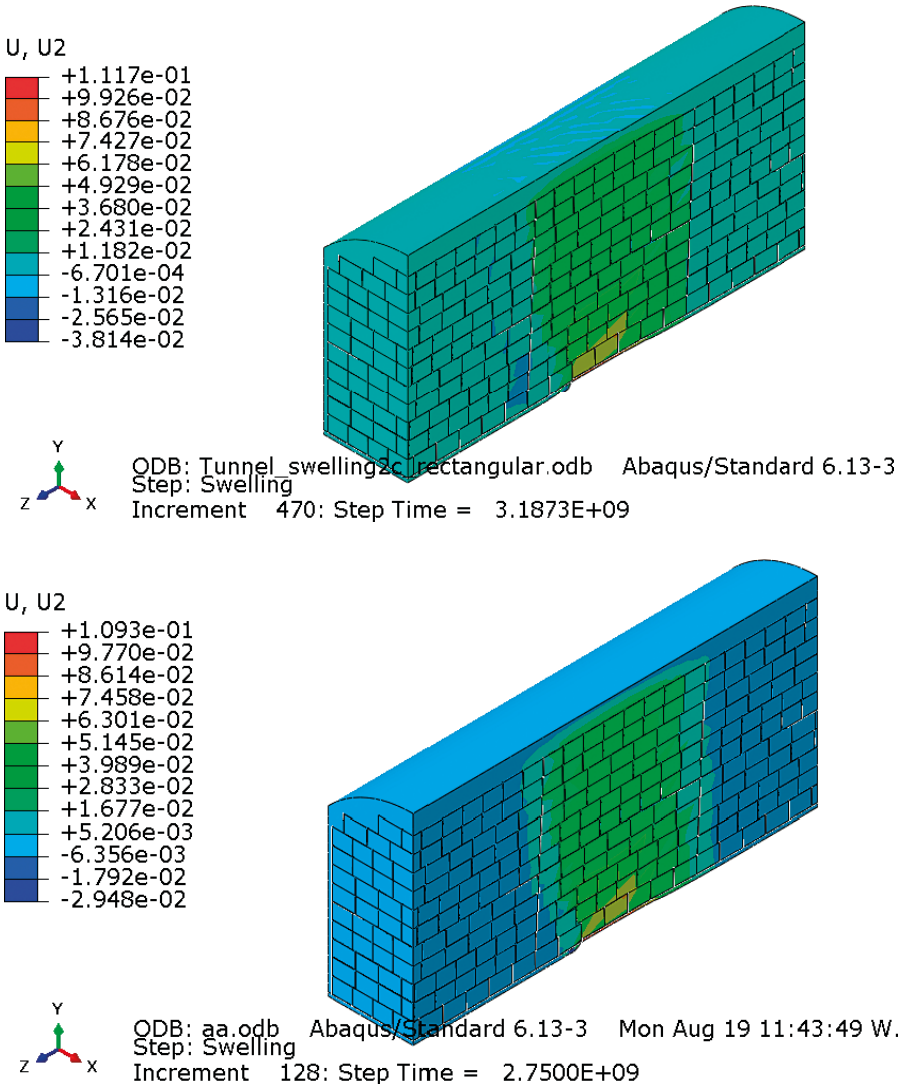

Figure 3-7. *Vertical displacements in the backfill. Upper rectangular bevel. Lower triangular bevel.*

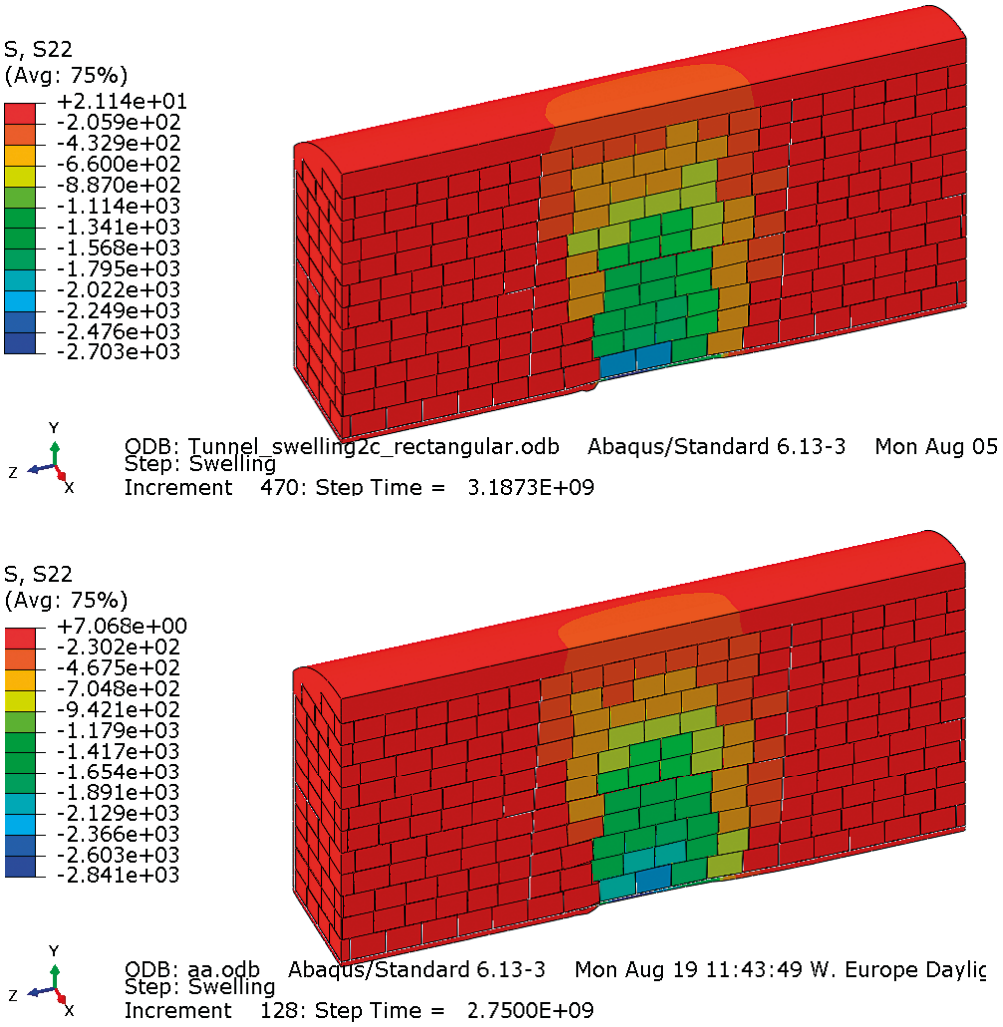

Figure 3-8. *Vertical stresses in the backfill (kPa). Upper rectangular bevel. Lower triangular bevel.*

History plots of the displacements in three points are shown in Figures 3-9 and 3-10. Figure 3-9 shows the vertical heave in the centre line of the deposition hole at the contact between the bentonite in the deposition hole and the backfill. It also shows the horizontal swelling into the bevel about 65 cm below the tunnel floor at the contact between the bentonite in the deposition hole and the pellets in the bevel.

The canister is also affected by the swelling and heaves about half a cm. Figure 3-10 shows the history plot.

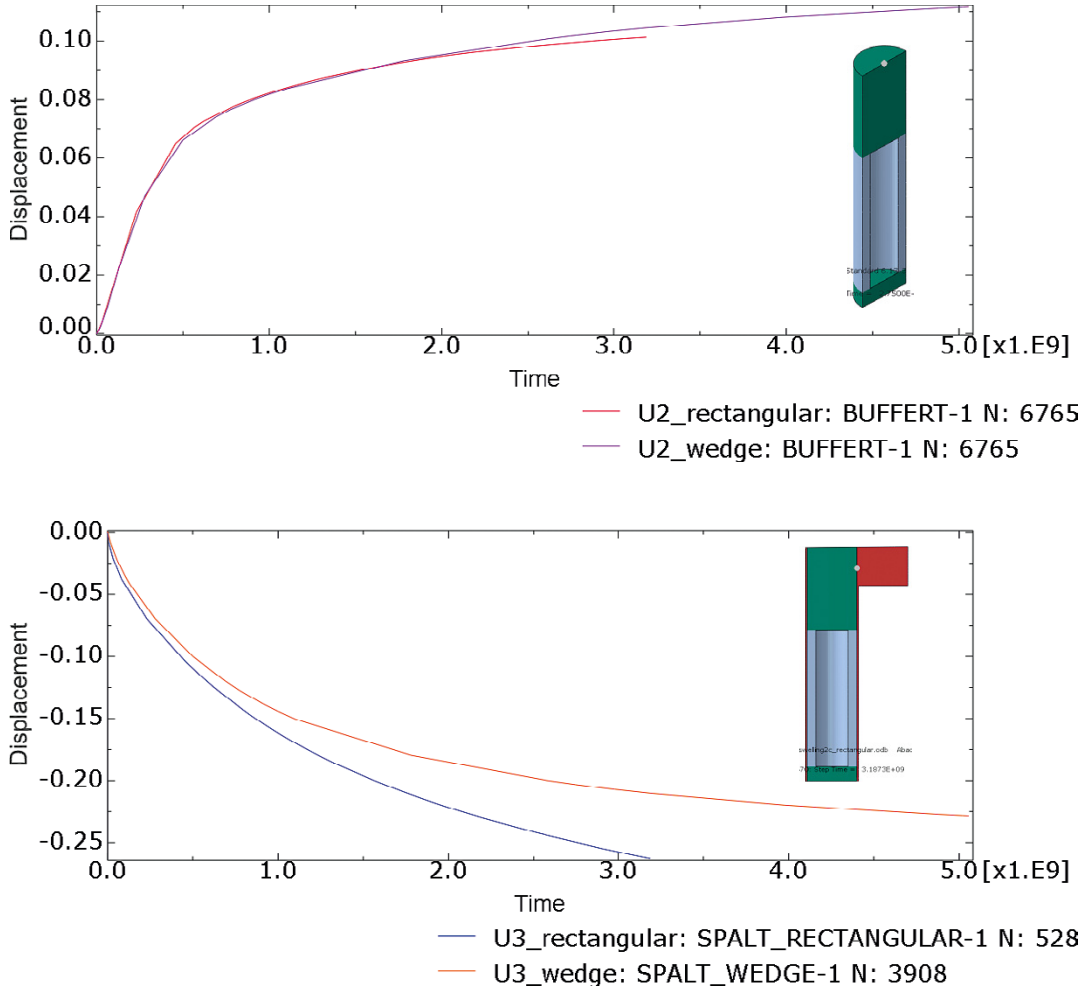

Figure 3-9. *Vertical displacements (m) in the contact between the bentonite in the deposition hole and the backfill (as illustrated) as a function of time (s); upper picture. Horizontal displacements (m) in the contact between the bentonite in the deposition hole and the pellets in the bevel (as illustrated) as a function of time (s); lower picture.*

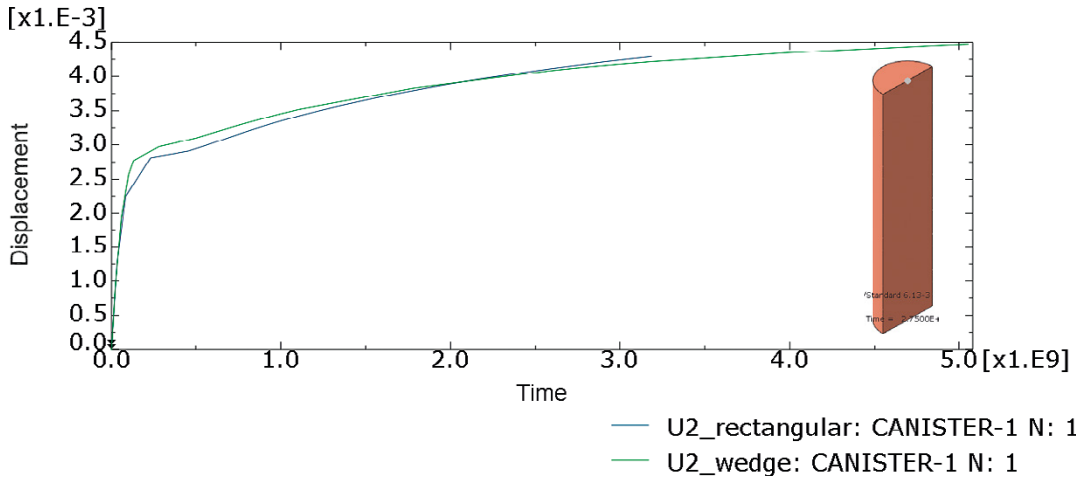

Figure 3-10. *Vertical upwards displacement (m) of the canister as a function of time (s).*

3.3 Influence of a remaining suction

The comparison between the two cases is based on the results at a small remaining suction of about 150 kPa. In order to assure that a small remaining suction has a very small influence on the results we can compare the results at the remaining suction 150 kPa with the results at the end of the calculation at a remaining suction of 60 kPa as shown in Figure 3-11. The elapsed time at the end of that calculation is about 5×10^9 seconds or 158 years or almost double the elapsed time at the time for the comparison which was about 3×10^9 seconds or 95 years. The very long time at the end of the calculations is caused by the low water pressure in the rock which has been set to 0 kPa.

Figure 3-12 shows comparison of the vertical displacements, Figure 3-13 comparison of the horizontal displacements and Figure 3-14 comparison of the vertical stresses.

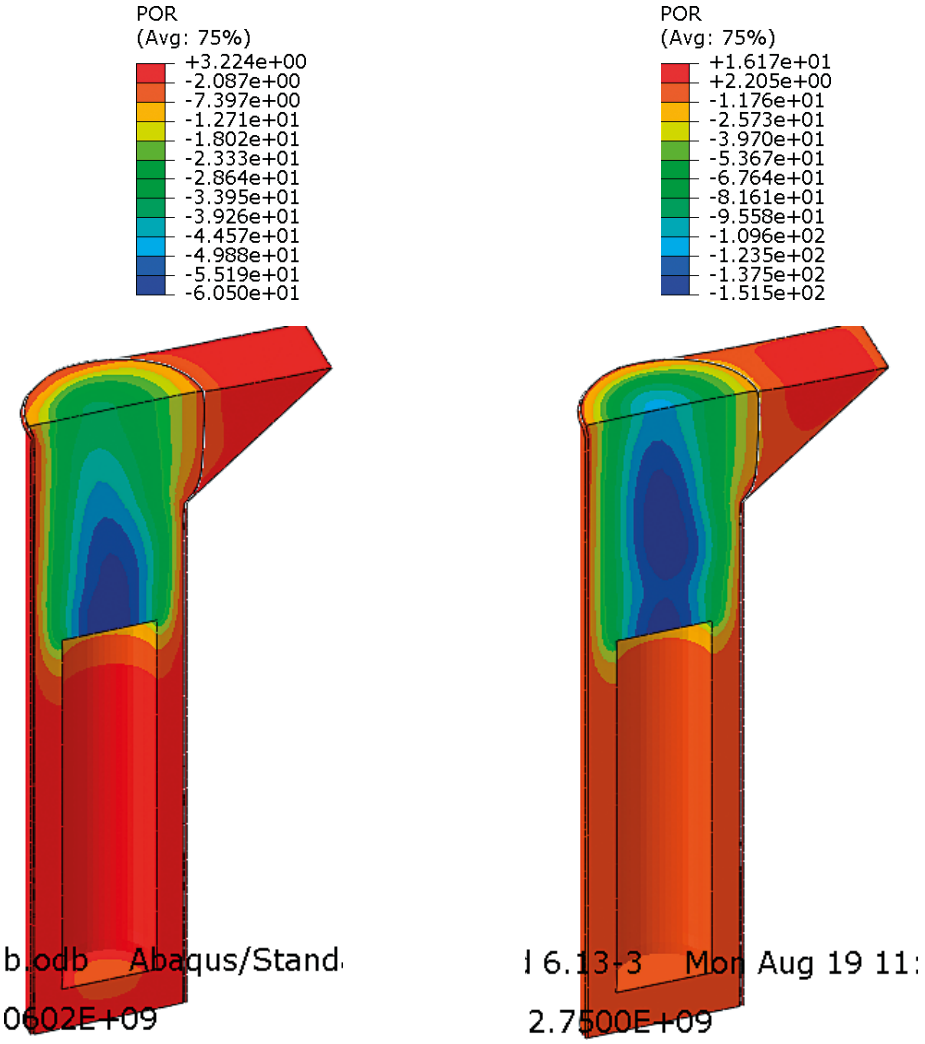

Figure 3-11. *Remaining pore water pressure distribution (kPa) at the time when the comparison is done (right) and at the end of the calculation with the triangular bevel (left).*

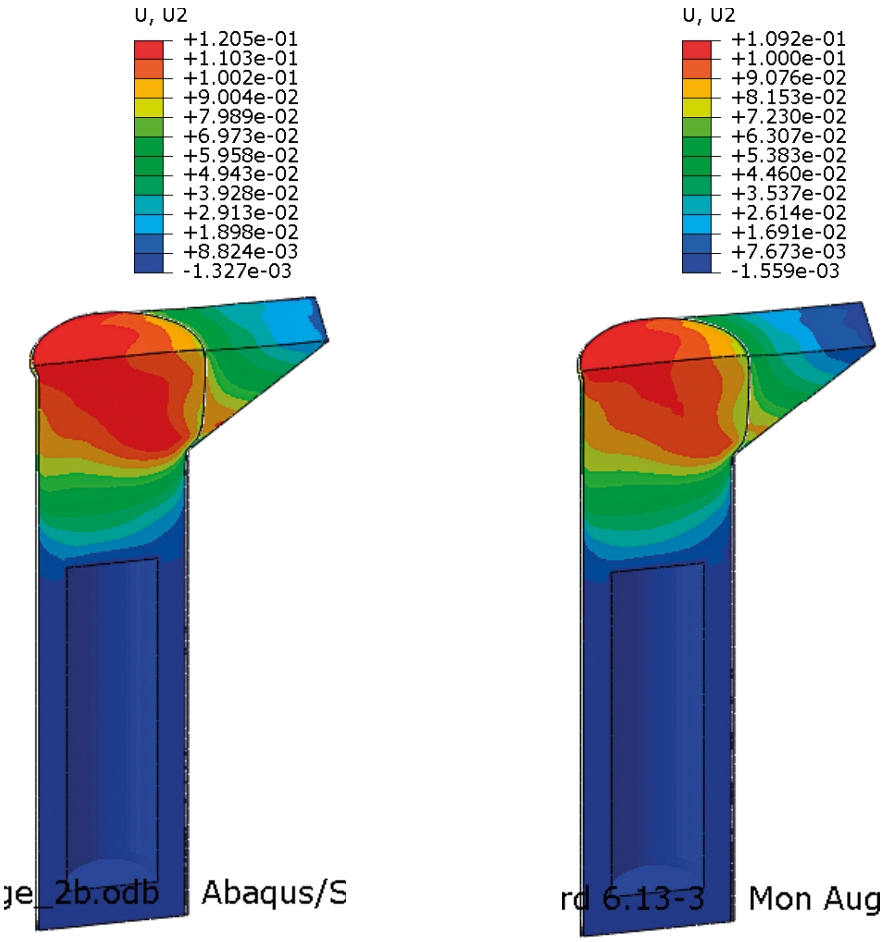

Figure 3-12. *Vertical displacements (m) at the time when the comparison is done (right) and at the end of the calculation (left).*

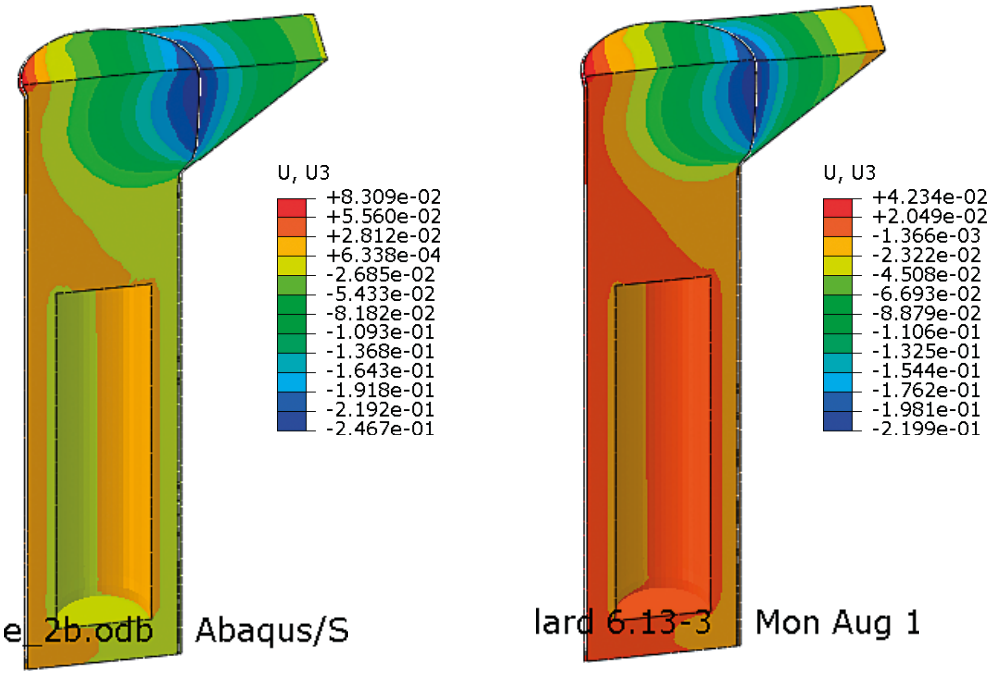

Figure 3-13. *Horizontal displacements (m) at the time when the comparison is done (right) and at the end of the calculation (left).*

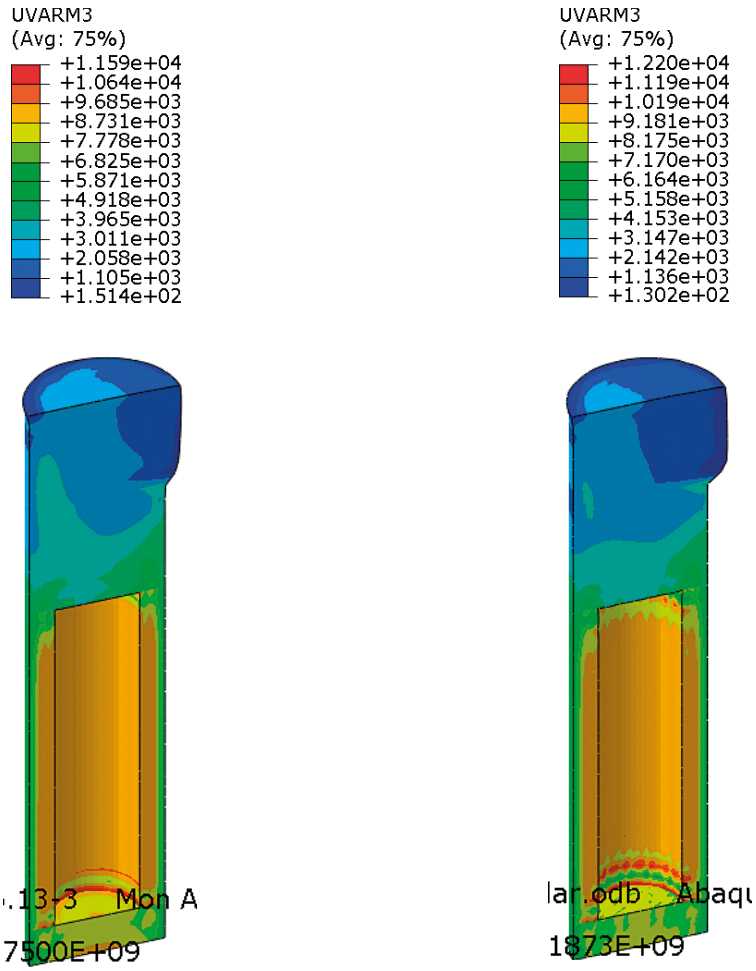

Figure 3-14. *Vertical stresses (kPa) in the deposition hole at the time when the comparison is done (right) and at the end of the calculation (left).*

The comparisons show that there is a small but obvious influence of the remaining suction. The displacements increase with about 10 % and the vertical stresses with about 13 % when reducing the remaining suction from 150 kPa to 60 kPa. However, this is judged not the influence the comparison that is done at the suction 150 kPa significantly since the comparison is made at equal suction.

4 Analyses and conclusions

The homogenisation and swelling of the bentonite in the deposition hole with an alternative design with a rectangular bevel has been modelled with Abaqus and compared to corresponding design with a triangular bevel. In the calculations all bentonite in the deposition hole and the bevel has been assumed to be water saturated from start but with the same dry density of the different components as planned to be installed. All bentonite in the tunnel has been assumed to stay dry and not be affected by wetting. This is an extreme case and the modelling is done in order to study a case that is assumed to be the worst possible scenario.

The calculations stopped before complete pore pressure equalisation due to convergence problems. The calculation regarding the new rectangular bevel stopped earlier than the one with triangular bevel. The reason is probably larger problems at the lower corner of the transition from the deposition hole to the bevel as can be seen in Figure 3-6 due to a sharper corner. The void ratio is very high at that corner.

The results of the calculations of the two bevel geometries are compared at the same remaining highest suction 150 kPa, which occurred at different times as shown in Figure 3-1.

The swelling into the rectangular bevel is as expected a little stronger than into the triangular one since the volume of low-density pellets is larger. The maximum horizontal swelling is 26 cm compared to 22 cm. This should result in a slightly lower density or higher void ratio in the upper part of the deposition hole. This is also the case as can be seen in Figures 3-5 and 3-6. It should also result in a slightly lower vertical stress between the bentonite in the deposition hole and the tunnel, which is also the case as can be seen by the highest stress on the backfill in Figure 3-8 (2.7 MPa compared to 2.8 MPa).

It is also obvious that the results do not represent the final state since the swelling at the interfaces between the bentonite in the deposition hole and the bentonite in the bevel and the tunnel increases with about 10 % at a reduction in maximum suction from 150 kPa to 60 kPa. However, the comparison should anyway be relevant since we are very close to pore pressure equalization (suction reduced from 18 400 kPa to less than 160 kPa) and the comparison is made at the same remaining suction in the bentonite in the deposition hole for the two cases.

The results show that there is an effect of the change to a rectangular bevel, but it is small and not important for the resulting density of the bentonite in the deposition hole.

References

SKB's (Svensk Kärnbränslehantering AB) publications can be found at www.skb.com/publications.

Börgesson L, Hernelind J, 2018. Modelling of the mechanical interaction between the buffer and the backfill in KBS-3V. Modelling results 2015. SKB TR-16-08, Svensk Kärnbränslehantering AB.

Börgesson L, Johannesson L-E, Sandén T, Hernelind J, 1995. Modelling of the physical behaviour of water saturated clay barriers. Laboratory tests, material models and finite element application. SKB TR-95-20, Svensk Kärnbränslehantering AB.

Börgesson L, Åkesson M, Hernelind J, 2020. EBS TF – THM modelling. Homogenisation task. SKB P-18-05, Svensk Kärnbränslehantering AB.

Åkesson M, Kristensson O, Börgesson L, Dueck A, Hernelind J, 2010a. THM modeling of buffer, backfill and other system components. Critical processes and scenarios. SKB TR-10-11, Svensk Kärnbränslehantering AB.

Åkesson M, Börgesson L, Kristensson O, 2010b. SR-Site Data report. THM modeling of buffer, backfill and other system components. SKB TR-10-44, Svensk Kärnbränslehantering AB.

Arkitektkopia AB, Bromma, 2020

SKB is responsible for managing spent nuclear fuel and radioactive waste produced by the Swedish nuclear power plants such that man and the environment are protected in the near and distant future.

skb.se